The pH dependence of spectral induced polarization of silica sands: Experiment and modeling

Magnus Skold, André Revil, P. Vaudelet

The pH dependence of spectral induced polarization of silica sands: Experiment and modeling

M. Skold,[1] A. Revil,[1,2] and P. Vaudelet[3]

Received 10 April 2011; revised 10 May 2011; accepted 11 May 2011; published 30 June 2011.

[1] In electrolyte-saturated sands, the storage of electrical charges under an alternating electrical field (called "induced polarization") is responsible for a phase lag between the applied current and the resulting electrical field. Because a variety of polarization mechanisms exists in porous materials, the underlying physics of induced polarization is somehow unclear and the field data difficult to interpret quantitatively. Measurements at various pHs and salinities can be used to discriminate between different competing mechanisms at low frequencies (1 mHz-1 kHz) in porous media in the absence of electronic conductors. New experimental data point out that, in addition to the polarization of the Stern layer (the inner part of the electrical double layer coating the surface of the silica grains), there is another polarization mechanism possibly associated with a hopping process of the protons on the silica surface. We propose that such a process could follow a Grotthuss cooperation mechanism (as in ice) involving the bound water of the silica surface. Our data also rule out a mechanism based on the diffuse layer. The new polarization mechanism may be applied to quantifying induced-polarization data collected over acidic contaminant plumes. **Citation:** Skold, M., A. Revil, and P. Vaudelet (2011), The pH dependence of spectral induced polarization of silica sands: Experiment and modeling, *Geophys. Res. Lett.*, *38*, L12304, doi:10.1029/2011GL047748.

1. Introduction

[2] Induced Polarization (IP, performed either in the time or frequency domain) has received considerable attention recently in environmental geophysics because of its sensitivity to bacterial activity in porous media and has been applied to the characterization of contaminant plumes and permeability [e.g., *Binley and Kemna*, 2005]. Induced polarization consists of the measurement of an impedance and a phase lag and provides information that is complementary to DC electrical conductivity measurements. The impedance and the phase lag can be used to define a complex conductivity $\sigma^* = \sigma' + i\,\sigma''$ (where i is the pure imaginary number) measurable over a broad range of frequencies (typically from 1 mHz to 10 kHz).

[3] Generally, induced polarization measurements are evaluated in terms of empirical or semi-empirical models. However such an approach is not satisfactory. The problem with developing a quantitative interpretation of induced polarization data is associated with the existence of a variety of competing mechanisms, which may overlap in the frequency domain. In abiotic porous materials with no metallic particles and below 100 Hz, there are three mechanisms that have been envisioned in the literature: (i) the diffuse layer polarization [*Dukhin and Shilov*, 2002], (ii) the membrane polarization [*Tarasov and Titov*, 2007], and (iii) the Stern layer polarization [*Leroy et al.*, 2008; *Revil and Florsch*, 2010]. In recent studies, Revil and colleagues have argued for a dominating role of the Stern layer polarization below 1 kHz in sands and glass beads [*Revil and Florsch*, 2010; *Schmutz et al.*, 2010; *Vaudelet et al.*, 2011] with counterions like weakly sorbed sodium (sites >Si-O$^-$Na$^+$, where > represents the crystalline framework) being mobile along the mineral surface. In the present paper, we will show that another polarization mechanism may exist that is associated with a hopping process of the protons along the mineral surface (a so-called Grotthuss cooperation mechanism).

[4] In the present paper, we analyze how induced polarization of silica sands is influenced by the pH of NaCl electrolytes. *Lesmes and Frye* [2001] have already investigated the influence of both the pH, pore water composition, and salinity of water saturated sands upon the induced polarization response of silica sands. However, their data were never used to discriminate between competing mechanisms and were never related to a speciation model of the mineral water interface. We present below new experimental results and reanalyze some published data to look for the main mechanism responsible for the observed IP response.

2. Material and Methods

[5] We performed spectral induced polarization (SIP) measurements using the type of tank described by *Schmutz et al.* [2010]. The high-resolution impedance meter we used is described in detail by *Zimmermann et al.* [2008]. The plastic tanks were 29 cm long and 18 cm wide and were packed with 6,000 g of sand and 1,850 g aqueous solution resulting in a sand depth of approximately 7.5 cm. The sand was packed wet to avoid trapping air bubbles and was maintained fully saturated throughout the experiment by minimizing evaporation using a plastic film above the tank. The wet sand was compacted for 75 minutes at 8.3 kPa resulting in a final volume of approximately 3.85 liters and a porosity $\phi = 0.41$. According to Archie's law for this type of sand ($F = \phi^{-m}$ with $m = 1.3$–1.5), F ranges the range 3.2–3.8 with a mean value of 3.5 in agreement with the measured value using electrolytes at different salinities (F =3.6). The tanks were left for five days to reach thermodynamic equilibrium and the SIP response was measured at several times

[1]Colorado School of Mines, Department of Geophysics, Golden, Colorado, USA.
[2]Equipe Volcan, ISTerre, UMR 5559, CNRS, Université de Savoie, Le Bourget du Lac, France.
[3]Institut EGID, Université Bordeaux 3, Pessac, France.

0094-8276/11/2011GL047748

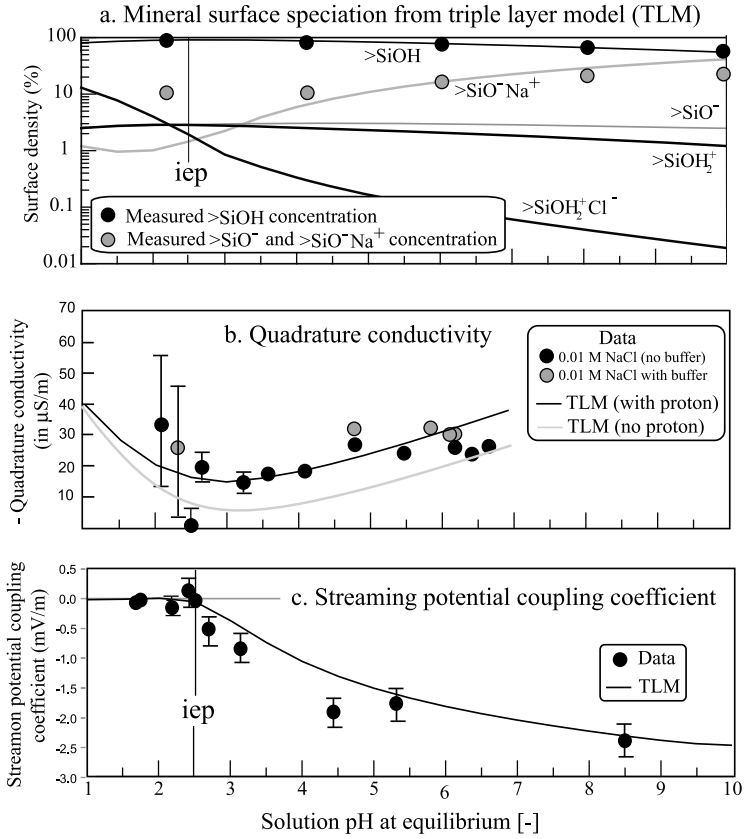

Figure 1. Influence of the pH on the surface speciation of silica, the quadrature conductivity, and the streaming potential coupling coefficient. (a) Speciation of the surface of silica at 0.01 M NaCl. The model is consistent with the surface composition of a quartz surface quantitatively evaluated using X-ray photoelectron spectroscopy [*Duval et al.*, 2002]. (b) Measured quadrature conductivity at 0.01 M NaCl (0.1 Hz). The error bars represent the standard deviation obtained from the phase measurement during three cycles at each frequency. The error bars are not visible when the symbols are larger than the error bars. The plain line corresponds to the contribution of the protons to the quadrature conductivity according to the model discussed in the main text. (c) Measured streaming potential coupling coefficient versus pH of the sand investigated in this work at equilibrium at 0.01 M NaCl. The plain line corresponds to the prediction of the Helmholtz-Smoluchowski equation with the zeta potential determined from the TLM approach. The result is independent of the existence of a transport mechanism for the protons along the mineral surface; iep stands for isoelectric point.

to assure that the electrical properties of the porous media were stable. Four non-polarizing Pb(s)/$PbCl_2$ electrodes were inserted 2 cm into the sand in a rectangular array with 8 and 10.5 cm long sides throughout the experiment. In all experiments, the Unimin #30 silica sand was used (effective grain size of 0.35 mm and 60% retention on mesh 40 sieve). Aqueous solutions were made by dissolving sodium chloride (Aldrich, ACS) into deionized water (DI). The pH of the NaCl solutions was adjusted with sodium hydroxide NaOH (Mallinckrodt Chemicals, ACS) or hydrochloric acid HCl (EMD Chemicals, ACS) prior to preparing the tanks. The NaCl concentration was kept constant at 0.01 mol L^{-1}. In the pH experiments, the initial pH of the NaCl solutions varied from 1.77 to 9.20. At the end of the experiments the pore water was separated from the sand and the pH and electrical conductivity of the fluid was measured with a combination electrode (WTW SenTix 41) and a conductivity meter from EXTECH (EC 500), respectively. During the experiment, the final pH became less acidic in solutions with original pH lower than 6 suggesting that mineral dissolution buffered the pH slightly. In some experiments, a pH buffer of 1 μmol L^{-1} acetic acid and 1 μmol L^{-1} potassium dihydrogen phosphate was used. This buffer does not affect the conductivity of the solution. Greater concentrations were not used for risk of affecting the SIP signal. The final pH ranged from 2.0 to 6.8 after 5 days.

[6] Duplicate experiments confirmed that the experimental procedure yielded repeatable results; the phase was within 5% between triplicate experiments at frequencies less than 10 Hz at neutral pH and 10 mM NaCl. The quadrature conductivity measurements carry greater uncertainty at lower pH values because of the greater fluid conductivities. The quadrature conductivity data are reported in Figure 1b at 0.1Hz. The SIP measurements were always performed at the final (equilibrium) pH in the frequency range 1 mHz-45 kHz.

[7] In addition to SIP measurements, we performed streaming potential measurements because of the streaming potential coupling coefficient is proportional to the zeta potential, a key-property of the electrical double layer [*Leroy et al.*, 2008]. We followed the same protocol as *Bolève et al.* [2007]. The pH at which the surface of the silica sand carries no diffuse layer, the so-called isoelectric point (iep), was determined by flushing a sand-filled column with 10 mM NaCl solutions at different pH while varying

Table 1. Equilibrium Constants for Surface Complexes From *Duval et al.* [2002] Used for the TLM Calculations

Reactions	Equilibrium Constants
$>SiOH + H^+ \leftrightarrow >SiOH_2^+$	$K_{>SiOH_2^+} = K_1 = 10^{1.0}$
$>SiOH \leftrightarrow >SiO^- + H^+$	$K_{>SiO^-} = K_2 = 10^{-4.0}$
$>SiO^- + Na^+ \leftrightarrow >SiO^-Na^+$	$K_{>SiO^-Na^+} = K_3 = 10^{1.7}$
$>SiOH_2^+ + Cl^- \leftrightarrow >SiOH_2^+Cl^-$	$K_{>SiOH_2^+Cl^-} = K_4 = 10^{1.8}$

the hydraulic gradient. A 50 cm long acrylic column with an inner diameter of 10.2 cm was filled with silica sand (Unimin #30). The column was packed wet to avoid air entrapment and the total porosity was 43.7%. Non-polarizing Ag(s)/AgCl electrodes were installed at the bottom and the top of the column to measure the streaming potential and therefore the streaming potential coupling coefficient. The results are presented in Figure 1c. Manometers were installed on the column at the same elevations as the electrodes so that the hydraulic gradient could be determined. The system was allowed to equilibrate for 3 days prior to flushing the column. For each NaCl solution at a given pH, approximately 40 liters of solution were flushed through the column. The influent and effluent pH typically differed 0.02 pH units or less.

3. Modeling

[8] In a coarse sand, neglecting the surface conductivity contribution to the in-phase conductivity, the in phase and quadrature conductivities are given by *Leroy et al.* [2008] and *Revil and Florsch* [2010],

$$\sigma' = \frac{1}{F}\sigma_f, \tag{1}$$

$$\sigma''(\omega) = -\left(\frac{F-1}{F}\right)\left(\frac{4\Sigma_S}{d}\right)\left(\frac{\omega\tau_0}{1+\omega^2\tau_0^2}\right), \tag{2}$$

where F (dimensionless) is the electrical formation factor related to porosity by Archie's law $F = \phi^{-m}$, m is the cementation exponent (dimensionless), d (in m) is the grain diameter, ω is the angular frequency, σ_f is the conductivity of the pore water (in S m^{-1}), $\tau_0 = d_0^2/8D_{(+)}$ is the main relaxation time (in s), $D_{(+)}$ (in m^2 s^{-1}) is the diffusion coefficient of the counterions of the Stern layer coating the surface of the mineral (related to the mobility by the Nernst Einstein relationship), and Σ_S is the specific surface conductivity (in S) of the inner part of the electrical double layer (called the Stern layer). The extension of equation (2) to a multicomponent electrolyte is given by *Revil and Florsch* [2010, Appendix D].

[9] The speciation of silica, the quadrature conductivity, and the streaming potential coupling coefficient are plotted versus the pH of the solution at equilibrium in Figures 1a–1c, respectively. The speciation model we used is described in Table 1 and we use the Triple Layer Model (TLM) model described by *Leroy et al.* [2008] and *Vaudelet et al.* [2011] modified to account for the sorption of chloride. The other parameters for the TLM model are the integral capacities of the inner and outer parts of the Stern layer, which are equal to $C_1 = 1.0$ F m^{-2} and $C_2 = 0.2$ F m^{-2}, respectively, and Γ_0 the total site density of the surface of silica is taken equal to 5 sites nm^{-2} and the pH(iep) = 2.5 [see *Duval et al.*, 2002]. The hydroxyl ions cannot be adsorbed on the surface of silica for the following reason: there is no OH^- in the pore water solution at low pHs while sorption of anions take place below the isoelectric point. The quadrature conductivity shows an increase below the isoelectric point, which is associated with both the sorption of Cl^- in the Stern layer and the existence of an alternative mechanism possibly associated with the hopping of protons along the mineral surface [see *Revil et al.*, 1999; *Leroy et al.*, 2008]. The specific surface conductivity of the Stern layer (in S) is defined by,

$$\Sigma^S = \int_{\Delta}(\sigma(\chi) - \sigma_f)d\chi. \tag{3}$$

where Δ corresponds to the thickness of the Stern layer, $\sigma(\chi)$ is the local conductivity at distance χ from the mineral surface, and σ_f is the conductivity of the bulk pore water. In the classical Triple Layer Model (TLM) approach, the Stern layer contribution comprises only the cations or anions sorbed to the mineral surface [e.g., *Leroy et al.*, 2008; *Vaudelet et al.*, 2011]. We will see below that another contribution is needed to fit the data, more precisely a contribution associated with mobile protons along the mineral surface.

[10] Figure 2 shows the TLM computation of the specific conductivity of the Stern layer versus the conductivity of the NaCl solution. The curve shown in Figure 2 corresponds to the prediction of the TLM adding a potential contribution to the specific surface conductivity of the Stern layer possibly associated with the migration of protons along the mineral surface:

$$\Sigma_S = \Sigma^S(Na^+) + \Sigma^S(Cl^-) + \Sigma^S(H^+). \tag{4}$$

[11] In equation (4), the first contribution comes from the sorption of Na^+ in the Stern layer (see details by *Leroy et al.* [2008], *Revil and Florsch* [2010], and *Vaudelet et al.* [2011]). This contribution dominates at high pH (pH > 4, see Figure 2a). The second contribution comes from the sorption of chloride on the mineral surface (see Table 1). The third contribution is associated with mobile protons as discussed in section 4. The two first contributions of the right-hand-side of equation (4) correspond to those shown in Figure 3a. According to Figure 1a, the surface reactions and their equilibrium constants determine which mechanism dominates at different pH ranges. The influence of the protons dominates only at very low pH values but does not seem to be negligible even at high pH values. This means that this contribution is important to characterize IP measurements performed over acidic contaminant plumes in the field.

[12] The contribution from the diffuse layer can be computed with the Bikerman equation,

$$\Sigma^d \approx 2\chi_d e\sum_{i=1}^{N} z_i\beta_i\left[\exp\left(-\frac{(\pm 1)ez_i\varphi_d}{2k_bT}\right) - 1\right], \tag{5}$$

(z_i the valence of species i is taken positive), φ_d is the inner potential of the electrical diffuse layer (in V), and N is the

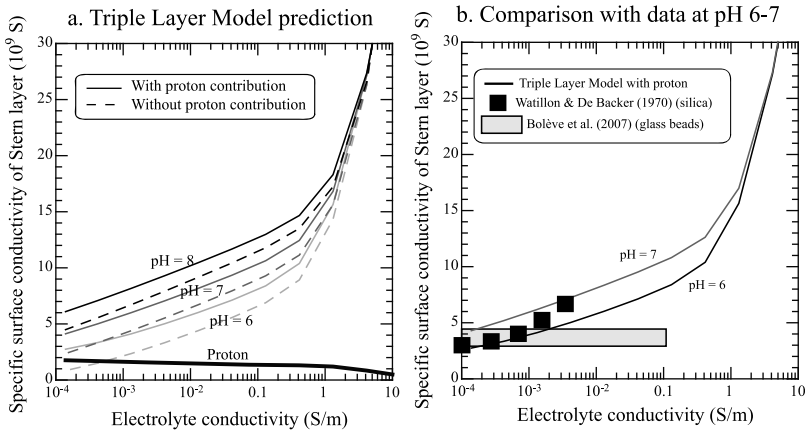

Figure 2. Dependence of the total specific surface conductivity of the Stern layer with the conductivity of the pore water solution. (a) TLM Computation for NaCl. The thick line for the protons comprises actually the results of the simulations at pH = 6, 7, and 8. (b) Comparison with experimental data at pH 6 and 7. Data from *Watillon and de Backer* [1970] (pH = 6.8, silica capillary) and *Bolève et al.* [2007] (pH = 5.6, glass beads). In both cases, the specific surface conductivity was derived from electrical conductivity measurements.

number of species present in the diffuse layer (e.g., $N = 4$ with Na^+, Cl^-, H^+, OH^-). The Debye screening length is defined by

$$\chi_d = \sqrt{\frac{\varepsilon_f k_b T}{2 I_f 10^3 N_A e^2}}, \tag{6}$$

where ε_f is the mean permittivity of the diffuse layer ($\varepsilon_f \approx 81 \times \varepsilon_0$, $\varepsilon_0 \approx 8.85 \times 10^{-12}$ F m^{-1}), T is the absolute temperature (in K), k_b is the Boltzmann constant (1.381×10^{-23} J K^{-1}), and I_f is the ionic strength of the pore water (usually expressed in mol L^{-1}),

$$I_f = \frac{1}{2}\sum_{i=1}^{N} z_i^2 C_i. \tag{7}$$

and N_A is the Avogadro number (6.02×10^{23} mol^{-1}) and C_i is the concentration of species i in the bulk pore water.

[13] Returning to the contribution of the protons to the Stern layer conductivity, *Revil et al.* [1999] and *Leroy et al.* [2008] noted that an additional conduction mechanism is required to fit the data and was attributed to the mobility of protons along the mineral surface but this idea was not explored further. We assume below that the protons are provided by the surface sites $>SiOH_2^+$ for which the protons are mobile. A more precise mechanism will be described below in section 4. If the protons of these sites are indeed mobile, a low frequency alternating electrical field can produce an accumulation of the surface protons on one side of a silica grain in a way similar to the mechanism described by *Leroy et al.* [2008] and *Revil and Florsch* [2010] for counterions. We can write:

$$\Sigma^S(H^+) = e\beta(H^+)\Gamma_{>SiOH_2^+}. \tag{8}$$

where e is the elementary charge of the proton (1.6×10^{-19} C) and $\beta(H^+)$ is the effective mobility of the proton along the

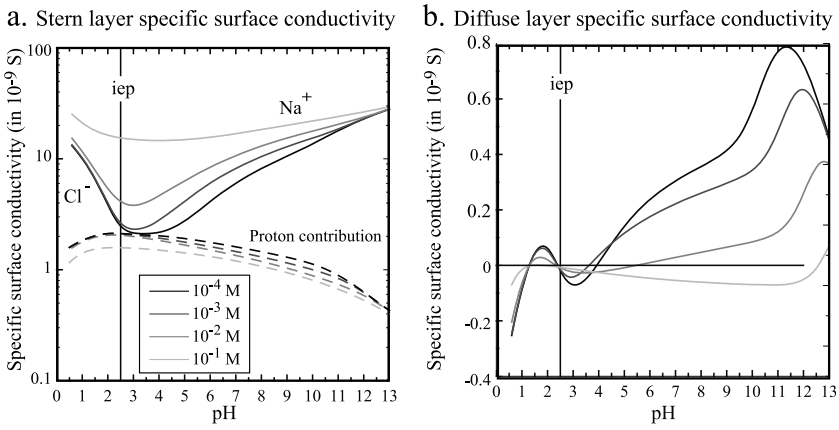

Figure 3. Triple Layer Model (TLM) computation of the specific surface conductivity of the Stern and diffuse layers (pH (iep)=2). (a) Specific surface conductivity of the Stern layer (in S) versus the pH at different salinities (NaCl). (b) Specific surface conductivity of the diffuse layer versus the pH at different salinities (NaCl). Note that at high salinities, the diffuse layer specific surface conductivity can be negative (there is a smaller conductivity in the diffuse layer by comparison with the bulk electrolyte).

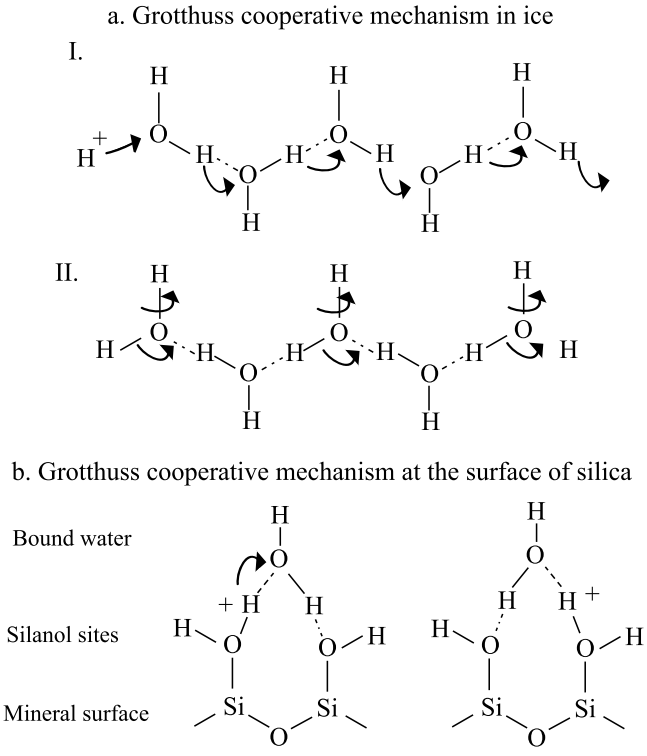

Figure 4. Proton conduction mechanism in ice and at the surface of silica. (a) Grotthuss cooperative mechanism for the diffusion of protons in ice [*Agmon*, 1995]. (b) Envisioned Grotthuss cooperative transport of the protons at the surface of silica. The surface conductivity associated with this hopping mechanism is proportional to the density of $>Si\text{-}OH_2^+$ surface sites, which is shown in Figure 1a.

mineral surface. We do not know how this mobility may change with the environmental parameters like the pH for instance. The value $\beta(H^+) = 9.0x10^{-8}$ $m^2s^{-1}V^{-1}$ at 25°C seems to explain the results reported in Figure 2b and those reported in Figure 1b. This value should be considered however with caution.

[14] The streaming potential coupling coefficient is modelled using the Helmholtz-Smoluchowski equation $C = (\delta\psi/\delta p)_{\mathbf{j}=0} = \varepsilon_f \zeta/(\eta_f \sigma_f)$ where ζ is the zeta potential (in V) (the double layer potential at the shear plane), ψ is the (macroscopic) streaming potential and η_f is the dynamic viscosity of the pore water (in Pa s). We use the classical approximation $\zeta = \varphi_d$ where φ_d is determined from the TLM.

[15] Note also that the diffuse layer specific surface conductivity (Figure 3b) is very small at small pH values (<4). Therefore a polarization model based entirely on the diffuse layer (as suggested in a broad number of publication in geophysics) can be ruled out as the dominating polarization mechanism.

4. Discussion

[16] We discuss below what polarization mechanism could be associated with the presence of protons along the silica surface. In order to understand the mechanism of proton transfer along the surface of silica, it is instructive to return to the Grotthuss-type cooperative transport of H^+ in ice. In Figure 4a, this mechanism is explained as the hopping of a proton first from the end of a H-bonded chain of water molecules to an adjacent group (right side of Figure 4a, top). The transfer of H-bond strength then allows it to be replaced by a H^+ binding on the other side. This yields to the geometry shown in Figure 4a (bottom). In the "rotational" phase, the rotation of the water molecules occurs as shown in Figure 4a (bottom) restoring the initial structure (Figure 4a, top). This so-called Grotthuss mechanism is therefore associated with the diffusion or electromigration of proton through the network of hydrogen bonds of water molecules through the formation or cleavage of covalent bonds.

[17] In a silicate rock, the water molecules involved in this H-bonded chain may be replaced by the silanol group as suggested in Figure 4b. The Grotthuss cooperative process is not an electromigration mechanism; the protons do not really move, they are just exchanged with the bound water, and therefore their positive charge is just hopping from site to site [*Daiko et al.*, 2004; *Schober*, 2006]. In an electrical field, we envision that the protons will move in the direction of the electrical field and would accumulate at the end of the grains. Then, they can diffuse back in their concentration gradient exactly as proposed for the sodium by *Leroy et al.* [2008] and *Revil and Florsch* [2010]. If this is correct, there is no DC-conductivity contribution from this Grotthuss cooperative process and therefore the protons do not control the streaming potential coupling coefficient. This mechanism will need to be explored further through molecular dynamic simulations in order to complete our understanding of the mechanisms of induced polarization in porous media.

5. Conclusions

[18] We have developed a speciation model for the surface of silica that is consistent with (1) with the surface composition of a quartz surface quantitatively evaluated using X-ray photoelectron spectroscopy (XPS) [*Duval et al.*, 2002], (2) quadrature conductivity data providing the total conductivity of the Stern layer, and (3) the determination of streaming potential coupling coefficient at different pH values. Precise SIP measurements points out that the classical Stern layer polarization mechanism cannot explain entirely the polarization of silica sands without adding an additional electrodiffusional mechanism associated with proton hopping along the silica surface through a Grotthuss cooperation mechanism. This mechanism may be associated with bound water molecules and the $>Si\text{-}OH_2^+$ sites. Molecular dynamic simulations are needed to test this assumption. This mechanism seems to explains qualitatively the available data and may be important in modelling the induced polarization response of acidic contaminant plumes.

[19] **Acknowledgments.** AR thanks the Office of Science (BER), US. Department of Energy, grant DE-FG02-08ER646559 for financial support. The PhD thesis of Pierre Vaudelet is supported by ADEME in France and the FEDER. We thank the two anonymous reviewers for their useful reviews of our manuscript.

[20] The Editor thanks two anonymous reviewers for their assistance in evaluating this paper.

References

Agmon, N. (1995), The Grotthuss mechanism, *Chem. Phys. Lett.*, *244*, 456–462, doi:10.1016/0009-2614(95)00905-J.

Binley, A., and A. Kemna (2005), DC resistivity and induced polarization methods, in *Hydrogeophysics*, edited by Y. Rubin and S. Hubbard, chap. 5, 129–156, Springer, Dordrecht, Netherlands, doi:10.1007/1-4020-3102-5_5.

Bolève, A., A. Crespy, A. Revil, F. Janod, and J. L. Mattiuzzo (2007), Streaming potentials of granular media: Influence of the Dukhin and Reynolds numbers, *J. Geophys. Res.*, *112*, B08204, doi:10.1029/2006JB004673.

Daiko, Y., T. Kasuga, and M. Nogami (2004), Pore size effect on proton transfer in sol–gel porous silica glasses, *Microporous Mesoporous Mater.*, *69*, 149–155, doi:10.1016/j.micromeso.2004.02.005.

Dukhin, S. S., and V. N. Shilov (2002), Non-equilibrium electric surface phenomena and extended electrokinetic characterization of particles, in *Interfacial Electrokinetics and Electrophoresis*, edited by A.V. Delgado, *Surfactant Sci. Ser.*, *106*, 55–85.

Duval, Y., et al. (2002), Evidence of the existence of three types of species at the quartz-aqueous solution interface at pH 0-10: XPS surface group quantification and surface complexation modeling, *J. Phys. Chem. B*, *106*, 2937–2945, doi:10.1021/jp012818s.

Leroy, P., A. Revil, A. Kemna, P. Cosenza, and A. Gorbani (2008), Spectral induced polarization of water-saturated packs of glass beads, *J. Colloid Interface Sci.*, *321*(1), 103–117, doi:10.1016/j.jcis.2007.12.031.

Lesmes, D. P., and K. M. Frye (2001), Influence of pore fluid chemistry on the complex conductivity and induced polarization responses of Berea sandstone, *J. Geophys. Res.*, *106*(B3), 4079–4090, doi:10.1029/2000JB900392.

Revil, A., and N. Florsch (2010), Determination of permeability from spectral induced polarization data in granular media, *Geophys. J. Int.*, *181*, 1480–1498, doi:10.1111/j.1365-246X.2010.04573.x.

Revil, A., L. M. Cathles, S. Losh, and J. A. Nunn (1998), Electrical conductivity in shaly sands with geophysical applications, *J. Geophys. Res.*, *103*(B10), 23,925–23,936, doi:10.1029/98JB02125.

Revil, A., P. A. Pezard, and P. W. J. Glover (1999), Streaming potential in porous media: 1. Theory of the zeta-potential, *J. Geophys. Res.*, *104*(B9), 20,021–20,031, doi:10.1029/1999JB900089.

Schmutz, M., et al. (2010), Influence of oil saturation upon spectral induced polarization of oil bearing sands, *Geophys. J. Int.*, *183*, 211–224, doi:10.1111/j.1365-246X.2010.04751.x.

Schober, T. (2006), Proton conductivity in silica gels, *Ionics*, *12*, 131–134, doi:10.1007/s11581-006-0028-0.

Tarasov, A., and K. Titov (2007), Relaxation time distribution from time domain induced polarization measurements, *Geophys. J. Int.*, *170*, 31–43, doi:10.1111/j.1365-246X.2007.03376.x.

Vaudelet, P., A. Revil, M. Schmutz, M. Franceschi, and P. Bégassat (2011), Induced polarization signatures of cations exhibiting differential sorption behaviors in saturated sands, *Water Resour. Res.*, *47*, W02526, doi:10.1029/2010WR009310.

Watillon, A., and R. de Backer (1970), Potentiel d'écoulement, courant d'écoulement et conductance de surface à l'interface eau-verre, *J. Electroanal. Chem. Interfacial Electrochem.*, *25*, 181–196.

Zimmermann, E., A. Kemna, J. Berwix, W. Glaas, H. M. Münch, and J. A. Huisman (2008), A high-accuracy impedance spectrometer for measuring sediments with low polarizability, *Meas. Sci. Technol.*, *19*, 105603. doi:10.1088/0957-0233/19/10/105603.

A. Revil and M. Skold, Colorado School of Mines, Department of Geophysics, Golden, CO 80401, USA. (arevil@mines.edu; mskold@mines.edu)

P. Vaudelet, Institut EGID, Université Bordeaux 3, F-33607 Pessac CEDEX, France. (pierre.vaudelet@gmail.com)